

# A Model for Blood Cell Transport and Separation in a Magnetophoretic Microsystem

E. P. Furlani

The Institute for Lasers, Photonics, and Biophotonics, University at Buffalo SUNY  
432 Natural Science Complex  
Buffalo, NY 14260-3000  
[efurlani@buffalo.edu](mailto:efurlani@buffalo.edu)

## ABSTRACT

We present a model for predicting the transport and separation of red and white blood cells in plasma in a magnetophoretic microsystem. The microsystem consists of an inlet that feeds a single microfluidic channel with multiple outlets. An array of integrated soft-magnetic elements is embedded adjacent to the microchannel, and once magnetized, these elements produce a magnetic force on blood cells as they flow through the channel. In whole blood, white blood cells (WBCs) behave as diamagnetic microparticles, while deoxygenated red blood cells (RBCs) exhibit paramagnetic behavior. We model the transport of these cells through the microsystem taking into account magnetic, fluidic and gravitational forces. Our analysis indicates that the microsystem is capable of separating WBCs, deoxygenated RBCs and plasma into respective outlets.

**Keywords:** blood cell magnetophoresis, magnetic blood cell separation, blood cell separation, micro total analysis system, magnetic bioseparation

## 1 INTRODUCTION

Microfluidic microsystems with magnetic functionality are finding increasing use in bioapplications for the controlled manipulation of biomaterials such as cells, enzymes, antigens and DNA [1]. In most such applications, the biomaterial needs to be magnetically “labeled” with surface bound magnetic micro/nano-particles in order to provide sufficient magnetic coupling to an applied field to enable manipulation. Direct manipulation (without labeling) is usually not possible because the magnetic susceptibility of most biomaterials is negligible. However, it is possible to manipulate blood cells directly [2,3]. In whole blood, white blood cells (WBCs) behave as paramagnetic microparticles, while deoxygenated red blood cells (RBCs) exhibit diamagnetic behavior. Thus, these two types of cells move in opposite directions in an applied field.

In this paper, we present a model for predicting the continuous and direct separation of blood cells in plasma in a magnetophoretic microsystem. The microsystem consists of an inlet that feeds a single microfluidic channel with

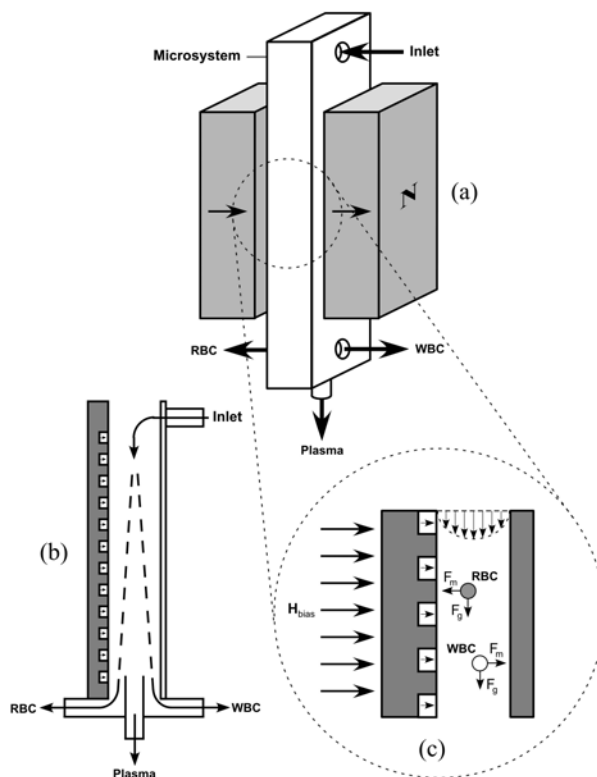


Figure 1: Magnetophoretic microsystem: (a) microsystem and bias magnets, (b) cross-section of microsystem showing magnetic elements and microchannel with outlets, and (c) magnified view of microfluidic channel showing the bias field, magnetic elements, and forces on red and white blood cells (RBCs and WBCs).

multiple outlets. An array of integrated soft-magnetic elements is embedded adjacent to the microchannel. A bias field is used to magnetize the elements, and once magnetized, these elements produce a magnetic force on blood cells as they flow through the microchannel. We present a model for predicting the motion of blood cells in the channel that takes into account magnetic, fluidic and gravitational forces. We use the model to study blood cell transport, and our analysis indicates that the microsystem is capable of separating WBCs, deoxygenated RBCs and cell-depleted plasma into respective outlets.

## 2 THEORETICAL MODEL

We predict the motion of blood cells in the microsystem using Newton's law,

$$m_c \frac{d\mathbf{v}_c}{dt} = \mathbf{F}_m + \mathbf{F}_f + \mathbf{F}_g, \quad (1)$$

where  $m_c$  and  $\mathbf{v}_c$  are the mass and velocity of the cell, and  $\mathbf{F}_m$ ,  $\mathbf{F}_f$ , and  $\mathbf{F}_g$  are the magnetic, fluidic and gravitational force (including buoyancy), respectively. The magnetic force is obtained using an "effective" dipole moment approach and is given by [3,4]

$$\mathbf{F}_m = \mu_0 V_c (\chi_c - \chi_f) (\mathbf{H}_a \cdot \nabla) \mathbf{H}_a, \quad (2)$$

where  $\chi_c$  and  $V_c$  are the susceptibility and volume of the cell, and  $\chi_f$  is the susceptibility of the transport fluid (in this case plasma).  $\mathbf{H}_a$  is the applied magnetic field at the center of the cell, and  $\mu_0 = 4\pi \times 10^{-7}$  H/m is the permeability of free space. The fluidic force is based on Stokes' law for the drag on a sphere in a viscous fluid,

$$\mathbf{F}_f = -6\pi\eta R_{c,hyd} (\mathbf{v}_c - \mathbf{v}_f), \quad (3)$$

where  $R_{c,hyd}$  is the effective hydrodynamic radius of the cell, and  $\eta$  and  $\mathbf{v}_f$  are the viscosity and the velocity of the fluid, respectively. The gravitational force is given by

$$\mathbf{F}_g = V_c (\rho_c - \rho_f) g \hat{\mathbf{x}}, \quad (4)$$

where  $\rho_c$  and  $\rho_f$  are the densities of the cell and fluid, respectively ( $g = 9.8$  m/s<sup>2</sup>). Note that gravity acts in the +x direction, parallel to the flow (see Figs. 1c and 2b).

### 2.1 Magnetic Force

The magnetic force depends on the field in the microchannel. This is a superposition of the bias field  $\mathbf{H}_{bias}$  and the field  $\mathbf{H}_e$  due to the array of magnetized elements,

$$\begin{aligned} \mathbf{H}_a &= \mathbf{H}_{bias} + \mathbf{H}_e \\ &= H_{e,x} \hat{\mathbf{x}} + (H_{bias,y} + H_{e,y}) \hat{\mathbf{y}}. \end{aligned} \quad (5)$$

These fields are not independent as  $\mathbf{H}_{bias}$  induces  $\mathbf{H}_e$ . The bias field can be optimized using an analytical formula, and once  $\mathbf{H}_{bias}$  is known we use a linear magnetization model with saturation to predict the magnetization  $\mathbf{M}_e$  of the soft-magnetic elements [5,6]. We assume that the elements are identical and noninteracting (i.e., the field of one does not affect the magnetization of another), and obtain

$$\mathbf{M}_e = \begin{cases} \frac{H_{bias}}{N_d} & H_{bias} < N_d M_{es} \\ M_{es} & H_{bias} \geq N_d M_{es} \end{cases}, \quad (6)$$

where  $N_d$  is the demagnetization factor of the element, which is geometry dependent, and  $M_{es}$  is its saturation magnetization [3].

Once  $\mathbf{M}_e$  is known,  $\mathbf{H}_e$  is easily determined. Specifically, the field solution for a long rectangular element of width  $2w$  and height  $2h$  that is centered with respect to the origin in the x-y plane, and magnetized parallel to its height (along the y-axis as shown in Fig. 2b) is well known (pp 210-211 in reference [7]).

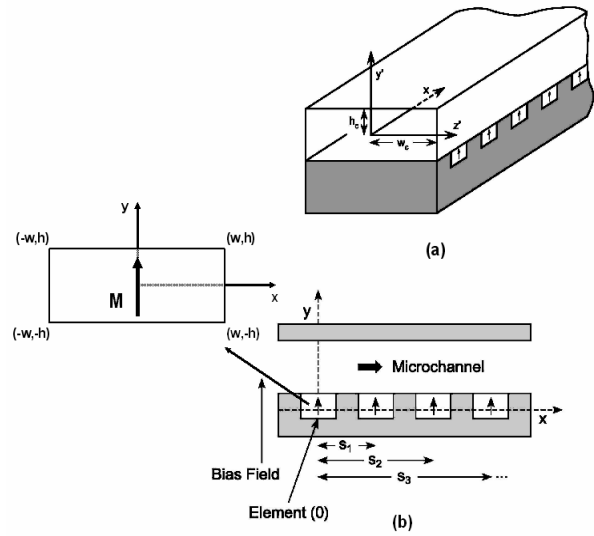


Figure 2: Magnetophoretic microsystem: (a) microfluidic channel, and (b) cross section of microsystem showing array of magnetized elements.

The field components are

$$H_{ex}^{(0)}(x, y) = \frac{M_e}{4\pi} \left\{ \ln \left[ \frac{(x+w)^2 + (y-h)^2}{(x+w)^2 + (y+h)^2} \right] - \ln \left[ \frac{(x-w)^2 + (y-h)^2}{(x-w)^2 + (y+h)^2} \right] \right\}, \quad (7)$$

and

$$H_{ey}^{(0)}(x, y) = \frac{M_e}{2\pi} \left\{ \tan^{-1} \left[ \frac{2h(x+w)}{(x+w)^2 + y^2 - h^2} \right] - \tan^{-1} \left[ \frac{2h(x-w)}{(x-w)^2 + y^2 - h^2} \right] \right\}. \quad (8)$$

In these equations,  $M_e$  is determined using Eq. (6).

The field due to the entire array of elements is obtained via superposition. Let  $N_e$  denote the number of elements, and let the first element be centered with respect to the origin in the x-y plane. All other elements are positioned along the x-axis as shown in Fig. 2b. We identify the elements using the index  $n = (0, 1, 2, 3, 4, \dots, N_e - 1)$ . The field components due to the first element ( $n = 0$ ) are given by Eqs. (7), (8). The  $n$ 'th element is centered at  $x = s_n$ , and its field and force components can be written in terms of the 0'th components as follows:

$$H_{ex}^{(n)}(x, y) = H_{ex}^{(0)}(x - s_n, y) \quad (n = 1, 2, 3, \dots) \quad (9)$$

$$H_{ey}^{(n)}(x, y) = H_{ey}^{(0)}(x - s_n, y).$$

The total field of the array is obtained by summing the contributions from all the elements,

$$H_{ex}(x, y) = \sum_{n=0}^{N_e-1} H_{ex}^{(0)}(x - s_n, y), \quad (10)$$

$$H_{ey}(x, y) = \sum_{n=0}^{N_e-1} H_{ey}^{(0)}(x - s_n, y). \quad (11)$$

The force components are given by [5,6]

$$\begin{aligned} F_{mx}(x, y) = & \mu_0 V_c (\chi_c - \chi_f) \left\{ \left( \sum_{n=0}^{N_e-1} H_{ex}^{(0)}(x - s_n, y) \right) \right. \\ & \times \left( \sum_{n=0}^{N_e-1} \frac{\partial H_{ex}^{(0)}(x - s_n, y)}{\partial x} \right) \\ & + \left( H_{bias,y} + \sum_{n=0}^{N_e-1} H_{ey}^{(0)}(x - s_n, y) \right) \\ & \left. \times \left( \sum_{n=0}^{N_e-1} \frac{\partial H_{ex}^{(0)}(x - s_n, y)}{\partial y} \right) \right\}, \quad (12) \end{aligned}$$

and

$$\begin{aligned} F_{my}(x, y) = & \mu_0 V_c (\chi_c - \chi_f) \left\{ \left( \sum_{n=0}^{N_e-1} H_{ex}^{(0)}(x - s_n, y) \right) \right. \\ & \times \left( \sum_{n=0}^{N_e-1} \frac{\partial H_{ey}^{(0)}(x - s_n, y)}{\partial x} \right) \\ & + \left( H_{bias,y} + \sum_{n=0}^{N_e-1} H_{ey}^{(0)}(x - s_n, y) \right) \\ & \left. \times \left( \sum_{n=0}^{N_e-1} \frac{\partial H_{ey}^{(0)}(x - s_n, y)}{\partial y} \right) \right\}. \quad (13) \end{aligned}$$

In Eqs. (12) and (13) we have assume that the bias field is constant and in the y-direction.

## 2.2 Fluidic Force

The fluidic force is based on Stokes' drag on a sphere. We assume fully developed laminar flow in the microchannel, and use a 1D approximation for the flow velocity profile. The, fluidic force is given by

$$\mathbf{F}_{fx} = -6\pi\eta R_{c,hyd} \left[ v_{c,x} - \frac{3\bar{v}_f}{2} \left[ 1 - \left( \frac{y - (h + h_c)}{h_c} \right)^2 \right] \right], \quad (14)$$

and

$$\mathbf{F}_{fy} = -6\pi\eta R_{c,hyd} v_{c,y}, \quad (15)$$

where  $h$  and  $h_c$  are the half-heights of the magnetic elements and channel, respectively (Fig. 2a),  $\bar{v}_f$  is the average fluid velocity, and  $R_{c,hyd}$  is the effective hydrodynamic radius of the cell.

## 2.3 Blood Cell Properties

The magnetic properties of white and red blood cells are needed to complete the mathematical model. White blood cells consist of five different types of cells that are classified into two groups: agranulocytes (lymphocyte and monocyte), and granulocytes (neutrophil, eosinophil and basophil). These five cell types have different sizes, with diameters that range from 6  $\mu\text{m}$  to 15  $\mu\text{m}$ . We account for these differences by using average WBC properties:  $\rho_{wbc} = 1070 \text{ kg/m}^3$ ,  $R_{wbc} = 5 \mu\text{m}$ , and  $V_{wbc} = 524 \mu\text{m}^3$ . White blood cells exhibit diamagnetic behavior in plasma, but their magnetic susceptibility is not well known. In order to model the behavior of these cells we use a lower bound estimate for WBC susceptibility, specifically we use the susceptibility of water  $\chi_{wbc} = -9.2 \times 10^{-6}$  (SI) [3].

Red blood cells, when unperturbed, have a well-defined biconcave discoid shape with a diameter of  $8.5 \pm 0.4 \mu\text{m}$  and a thickness of  $2.3 \pm 0.1 \mu\text{m}$ . These cells account for approximately 99% of the particulate matter in blood, and the percentage by volume (hematocrit) of packed red blood cells in a given sample of blood, is normally 40-45%. For red blood cells, we use  $R_{rbc} = 3.84 \mu\text{m}$  (hydrodynamic radius),  $V_{rbc} = 88.4 \mu\text{m}^3$ , and  $\rho_{rbc} = 1100 \text{ kg/m}^3$ . The susceptibility of a RBC depends on the oxygenation of its hemoglobin. We use  $\chi_{rbc,oxy} = -9.22 \times 10^{-6}$  (SI) and  $\chi_{rbc,deoxy} = -3.9 \times 10^{-6}$  (SI) for oxygenated and deoxygenated red blood cells, respectively [3]. Lastly, we use the following properties for blood plasma:  $\eta = 0.001 \text{ kg/s}$ ,  $\rho_f = 1000 \text{ kg/m}^3$  and  $\chi_f = -7.7 \times 10^{-6}$  (SI).

## 2.4 Equations of Motion

The equations of motion for blood cell transport through the microsystem can be written in component form by substituting Eqs. (12) - (15) into Eq. (1),

$$m_c \frac{dv_{c,x}}{dt} = F_{mx}(x_c, y_c) + V_c(\rho_c - \rho_f)g - 6\pi\eta R_{c,hyd} \left[ v_{c,x} - \frac{3\bar{v}_f}{2} \left[ 1 - \left( \frac{y - (h + h_c)}{h_c} \right)^2 \right] \right], \quad (16)$$

$$m_c \frac{dv_{c,y}}{dt} = F_{my}(x, y) - 6\pi\eta R_{c,hyd} v_{c,y}, \quad (17)$$

$$v_{c,x}(t) = \frac{dx_c}{dt}, \quad v_{c,y}(t) = \frac{dy_c}{dt}. \quad (18)$$

Equations (16) - (18) can be solved numerically, subject to initial conditions for  $x_c(0)$ ,  $y_c(0)$ ,  $v_{c,x}(0)$ , and  $v_{c,y}(0)$ .

## 3 SIMULATIONS

We use Eqs. (16) and (17) to study blood cell transport in a specific microsystem design. The microchannel in the system is  $120 \mu\text{m}$  high,  $1 \text{ mm}$  wide and  $35 \text{ mm}$  long. There are 76 identical permalloy elements (78% Ni 22% Fe,  $M_{es} = 8.6 \times 10^5 \text{ A/m}$  [7]) embedded adjacent to the channel. Each element is  $200 \mu\text{m}$  high and  $200 \mu\text{m}$  wide, and they are spaced  $200 \mu\text{m}$  apart (edge to edge). Thus, the elements span a distance of  $30.2 \text{ mm}$  along the channel. The bias field is  $H_{bias} = 3.9 \times 10^5 \text{ A/m}$  (5000 Gauss), which is sufficient to saturate the elements.

Venous blood containing WBCs and deoxygenated RBCs is introduced into the inlet. We assume that the blood cells enter the microchannel to the left of the first element at  $x(0) = -4w$ , and at various initial heights:  $y(0) = 115 \mu\text{m}$ ,  $130 \mu\text{m}$ , ...,  $205 \mu\text{m}$ . The top of the microchannel is  $120 \mu\text{m}$  above the elements at  $y = 220 \mu\text{m}$ . The average fluid velocity is  $\bar{v}_f = 0.2 \text{ mm/s}$ , and the cells enter the channel with a velocity that correlates with their height in the channel (laminar flow). We use Eqs. (16) and (17) to predict the WBC and RBC trajectories, which are shown in Fig. 3a and 3b, respectively. The trajectory profiles are irregular due to the spatial variation of the magnetic force [3]. Note that the WBCs and deoxygenated RBCs separate before they reach the end of the array. Specifically, all the WBCs move to the top of the channel, while all the deoxygenated RBCs move to the bottom. The separation times for the WBCs and RBCs (i.e. the time it takes for all of the cells to reach their respective ends of the microchannel) are 95s and 120s, respectively. At the end of the microchannel, WBCs and deoxygenated RBCs exit at respective outlets, while cell depleted plasma exits through the central outlet as shown in Fig. 1b.

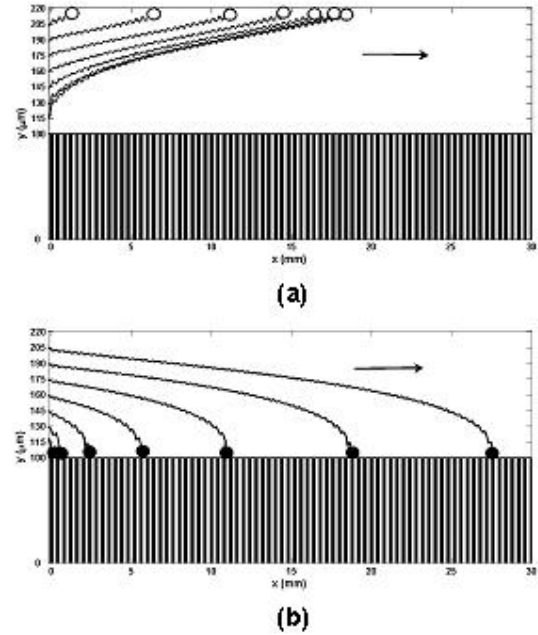


Figure 3. Predicted blood cell trajectories: (a) WBC trajectories, (b) deoxygenated RBC trajectories.

## 4 CONCLUSIONS

We have presented a passive magnetophoretic microsystem for separating blood cells, and a model for predicting its performance. We have used the model to study a blood cell transport, and our analysis indicates that the microsystem is capable of separating WBCs, deoxygenated RBCs and plasma into separate outlets.

## REFERENCES

- [1] M. A. M. Gijs "Magnetic bead handling on-chip: new opportunities for analytical applications," *Microfluidics and Nanofluidics*, 1(1):22-40, 2004.
- [2] K-H Han, and A. B. Frazier, "Diamagnetic Capture Mode Magnetophoretic Microseparator for Blood Cells," *J. Micromech. Sys.*, 14 (6) 1422-1431, 2005.
- [3] E. P. Furlani, "Magnetophoretic Separation of Blood Cells at the Microscale," *J. Phys. D: Appl. Phys.* **40** 1313-1319, 2007.
- [4] E. P. Furlani and K. C. Ng, "Analytical Model of Magnetic Nanoparticle Transport and Capture in the Microvasculature," *Phys. Rev. E* **73**, 061919, 2006.
- [5] E. P. Furlani and Y. Sahoo, "Analytical Model for the Magnetic Field and Force in a Magnetophoretic Microsystem," *J. Phys. D: Appl. Phys.* **39** 1724-1732, 2006.
- [6] E. P. Furlani, "Analysis of Particle Transport in a Magnetophoretic Microsystem," *J. Appl. Phys.* **99**, 2006.
- [7] E. P. Furlani, *Permanent Magnet and Electromechanical Devices; Materials, Analysis and Applications*, Academic Press, NY, 2001.